

Comprehensive Approach to the Profiling of the Cooked Meat Carcinogens 2-Amino-3,8-dimethylimidazo[4,5-*f*]quinoxaline, 2-Amino-1-methyl-6-phenylimidazo[4,5-*b*]pyridine and their Metabolites in Urine of Meat-Eaters

*Dan Gu*¹, *Lynn McNaughton*², *David Le Master*², *Brian G. Lake*³, *Nigel J. Gooderham*⁴, *Fred Kadlubar*⁵,

and Robert J. Turesky^{1,*}

¹Division of Environmental Health Sciences and ²Division of Translational Medicine, Wadsworth Center, New York State Department of Health, Albany, New York 12201

³ Centre for Toxicology, Health and Medical Sciences, University of Surrey, GU2 7XH, UK and LFR Molecular Sciences, Randalls Road, Leatherhead, Surrey, KT22 7RY, UK

⁴Biomolecular Medicine, Faculty of Medicine, Imperial College London, Sir Alexander Fleming Building, London SW7 2AZ, United Kingdom.

⁵ Winthrop P. Rockefeller Cancer Institute, University of Arkansas for Medical Sciences, Little Rock, AR 72205

Supporting Information

Table S-1. Chemical Shift Data (ppm) for PhIP-*N*-glucuronides

Table S-2. Performance of the analytical method for PhIP and its metabolites.

Figure S-1A 2D ^1H - ^1H COSY NMR spectra of PhIP-*N*²-G1 and PhIP-*N*3-G1

Figure S-1B 2D ^1H - ^1H COSY NMR spectra of PhIP-*N*3-G1 (downfield region)

Figure S-1C 2D ^1H - ^1H COSY NMR spectra of PhIP-*N*3-G1 (upfield region)

Figure S-2A – S-2C. Calibration curves of MeIQx and its metabolites

Figure S-3A – S-3D Calibration curves of PhIP and its metabolites

Figure S-4. LC-ESI/MS/MS traces of MeIQx, PhIP, and 4-OH-PhIP in urine of an omnivore, before and after acid hydrolysis of urine.

Table S-1. Chemical Shift Data (ppm) for PhIP-*N*-glucuronides

Chemical Shift Data (ppm) for Rabbit and Human Liver PhIP-glucuronides

Position	Rabbit (PhIP-<i>N</i>²-GI)	Human (PhIP-<i>N</i>³-GI)
N-CH ₃	3.58	3.46
NH	7.81	not detected
4'-H	7.29	7.38
3',5'-H	7.42	7.48
2',6'-H	7.66	7.70
5	8.30	8.22
7	7.80	7.75
1''	5.02	5.54
2''	3.34	4.51
3''	3.25	3.40
4''	3.23	3.50
5''	3.48	3.62

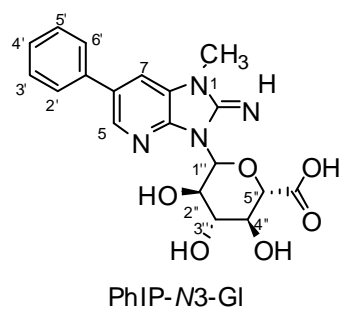
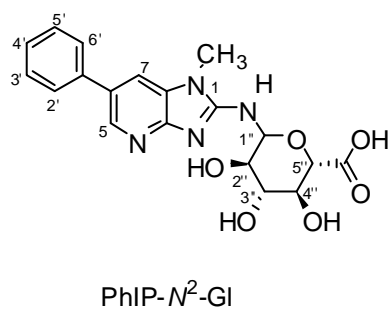


Table S-2. Performance of the analytical method for PhIP and its metabolites.

Subject	Metabolite		Amount (pg/mL)			Overall mean	CV(%) within-day	CV(%) between-day
			Day 1	Day 2	Day 3			
9	HON-PhIP- <i>N</i> ² -GI	Mean	1020	968	943	977	3.3	4.9
		SD	49.1	17.5	18.2			
		RSD(%)	4.8	1.8	1.9			
	HON-PhIP- <i>N</i> ₃ -GI	Mean	105	92.2	91.8	96.2	5.2	8.4
		SD	2.9	3.1	7.4			
		RSD(%)	2.8	3.4	8.1			
	PhIP	Mean	9.7	8.9	9.4	9.3	8.2	7.8
		SD	0.3	0.9	1.0			
		RSD(%)	3.2	9.8	10.1			
14	HON-PhIP- <i>N</i> ² -GI	Mean	723	726	681	710	1.9	3.5
		SD	13.6	6.1	17.9			
		RSD(%)	1.9	0.8	2.6			
	HON-PhIP- <i>N</i> ₃ -GI	Mean	45.4	43.7	48.2	45.8	4.3	6.1
		SD	2.2	1.6	2.1			
		RSD(%)	4.8	3.7	4.4			
	PhIP	Mean	4.8	4.7	4.8	4.8	7.0	5.9
		SD	0.3	0.4	0.4			
		RSD(%)	6.3	8.5	8.3			
20	HON-PhIP- <i>N</i> ² -GI	Mean	1438	1291	1302	1344	4.2	7.1
		SD	83.7	11	43			
		RSD(%)	5.8	0.9	3.3			
	HON-PhIP- <i>N</i> ₃ -GI	Mean	147	147	151	148	3.4	3.2
		SD	6.1	3.5	5			
		RSD(%)	4.1	2.4	3.3			
	PhIP	Mean	10.9	11	11.3	11.1	6.7	5.9
		SD	0.5	1	0.6			
		RSD(%)	4.6	9.1	5.3			

n = 3 or 4 replicates per day

Double quantum filtered 2D ^1H - ^1H COSY NMR spectra of the rabbit liver and human liver microsomal metabolites in $\text{DMSO-}d_6$ are shown in Figure S-1. In panel A, the spectrum of the rabbit liver microsomal metabolite illustrates a crosspeak between the anomeric H^1 and the exocyclic imine proton on N^2 , confirming the glucuronide linkage at this site as anticipated for $\text{PhIP-}N^2\text{-Gl}$. Addition of $^2\text{H}_2\text{O}$ leads to the selective loss of the exocyclic imine ^1H resonance. The spin coupling connectivities for the aromatic ^1H resonances are indicated. In panel B is illustrated the analogous spectral region for the human liver microsomal metabolite. No spin coupling or dipolar coupling interaction was observed between the glucuronide ring and the aromatic rings of this metabolite. The absence of an additional spin coupling to the anomeric proton is consistent with the structure of the conjugate being a tertiary amine-linked PhIP glucuronide moiety. In panel C, spin coupling correlations between all of the protons in the $\text{PhIP-}N^3\text{-Gl}$ glucuronide ring are observed, thus allowing for the complete assignment of these resonances (1). Combined with the assignment of the aromatic proton spectrum, these spectral data are compatible with the $\text{PhIP-}N^3\text{-Gl}$ structure.

Figure S-1A. 2D ^1H - ^1H COSY NMR spectra of $\text{PhIP-}N^2\text{-Gl}$

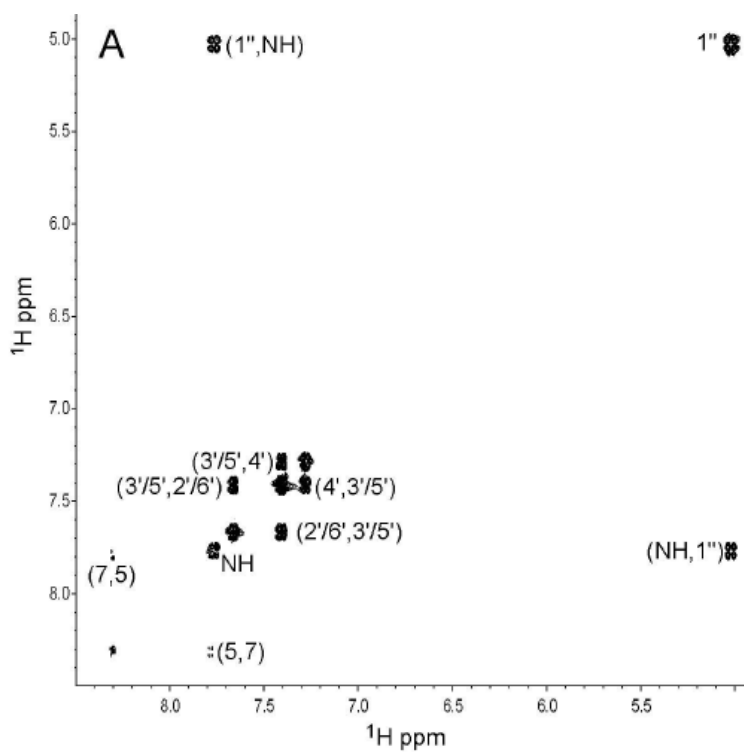


Figure S-1B. 2D ^1H - ^1H COSY NMR spectra of PhIP-*N*3-G1 (downfield region)

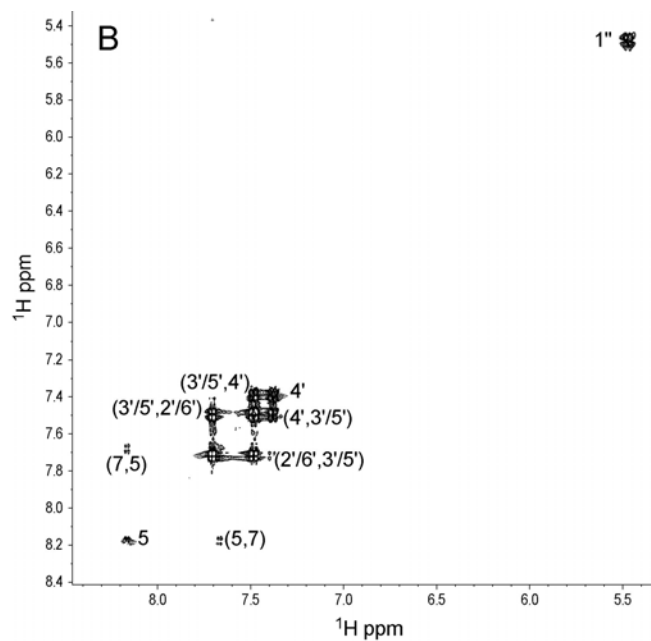


Figure S-1C. 2D ^1H - ^1H COSY NMR spectra of PhIP-*N*3-G1 (upfield region)

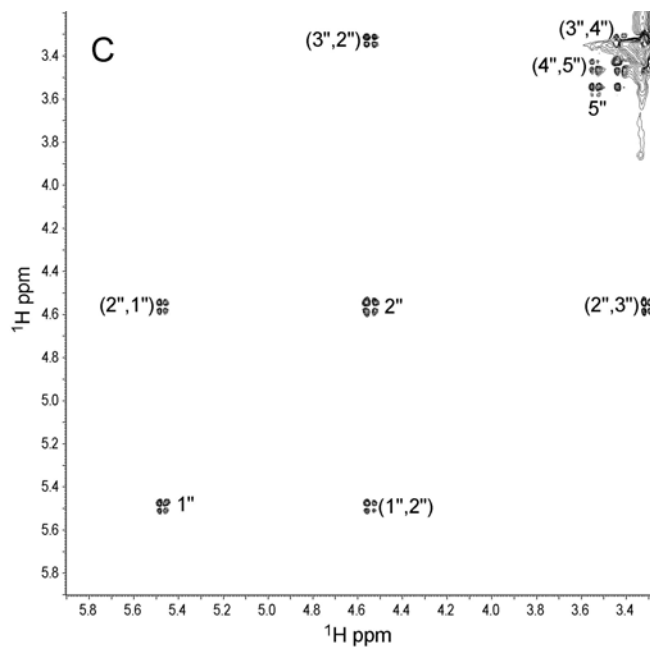


Figure S-2A – S-2C. Calibration curves of MeIQx and its metabolites

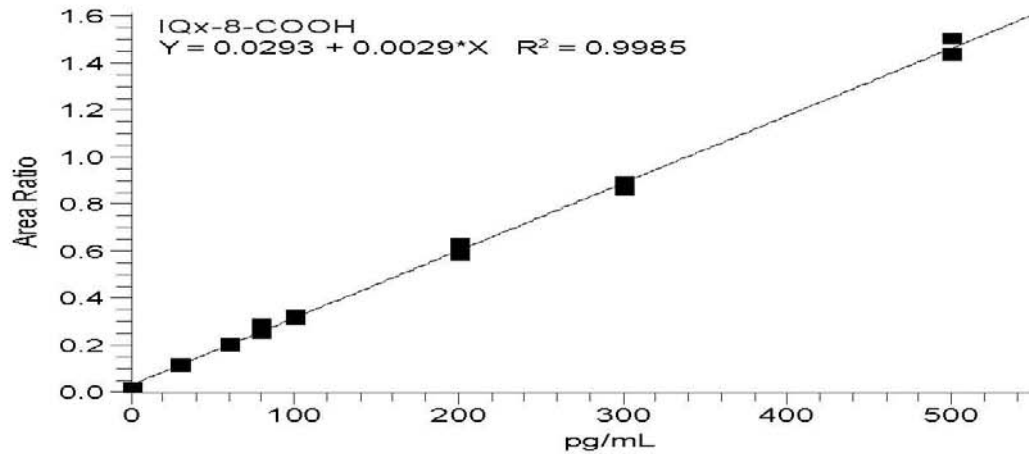
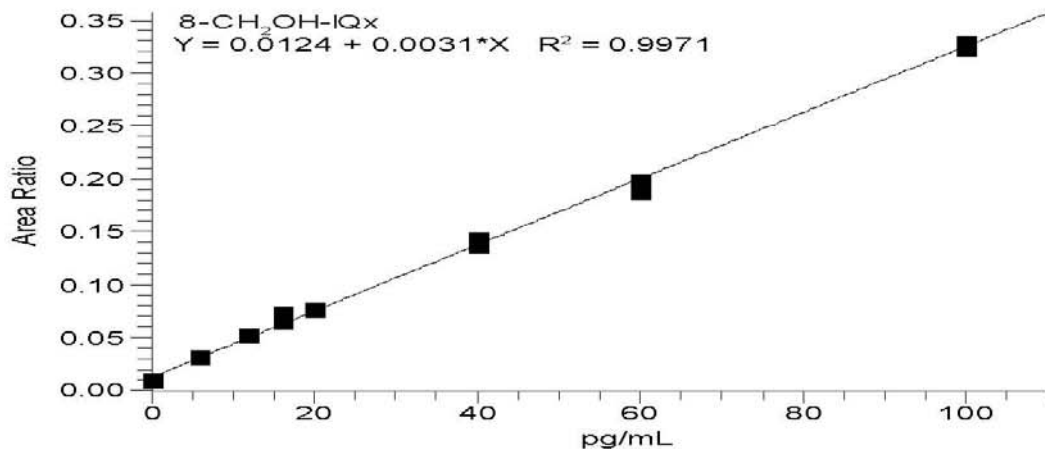
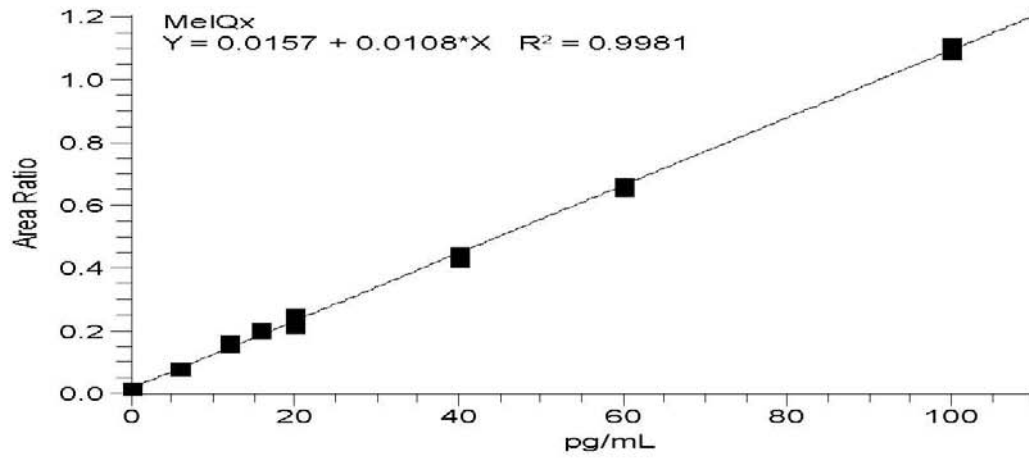
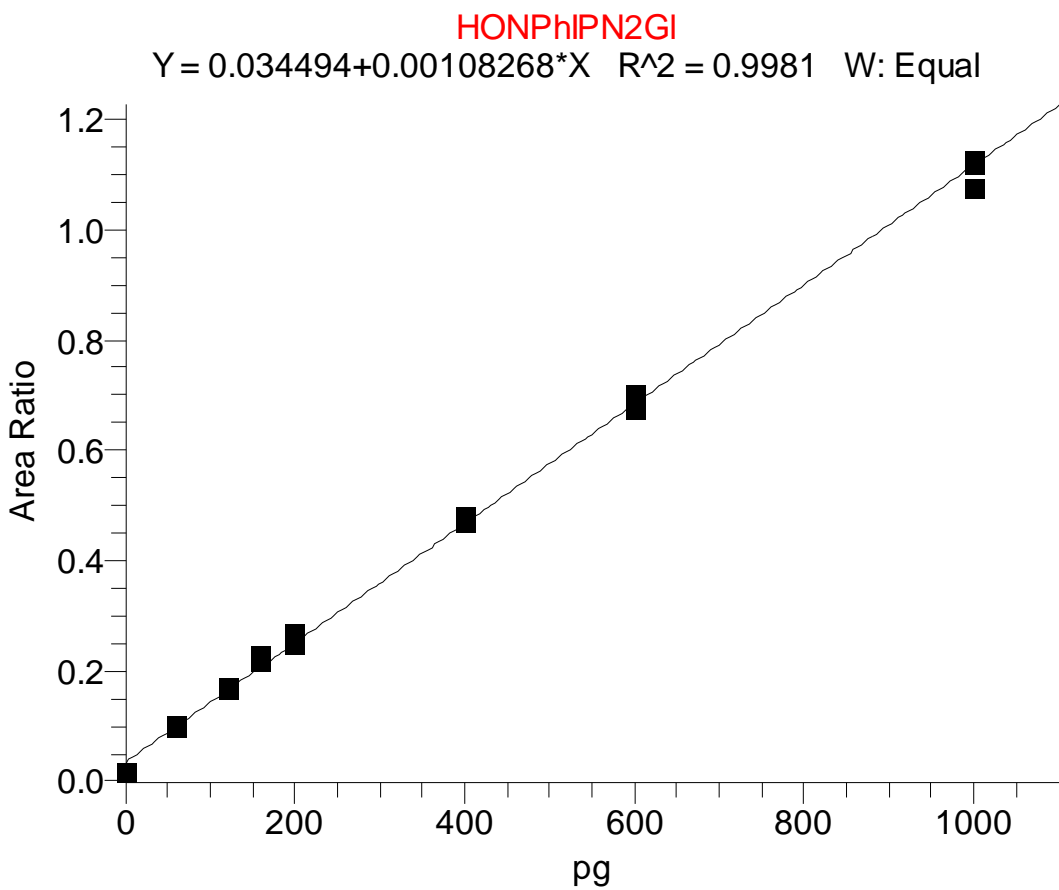
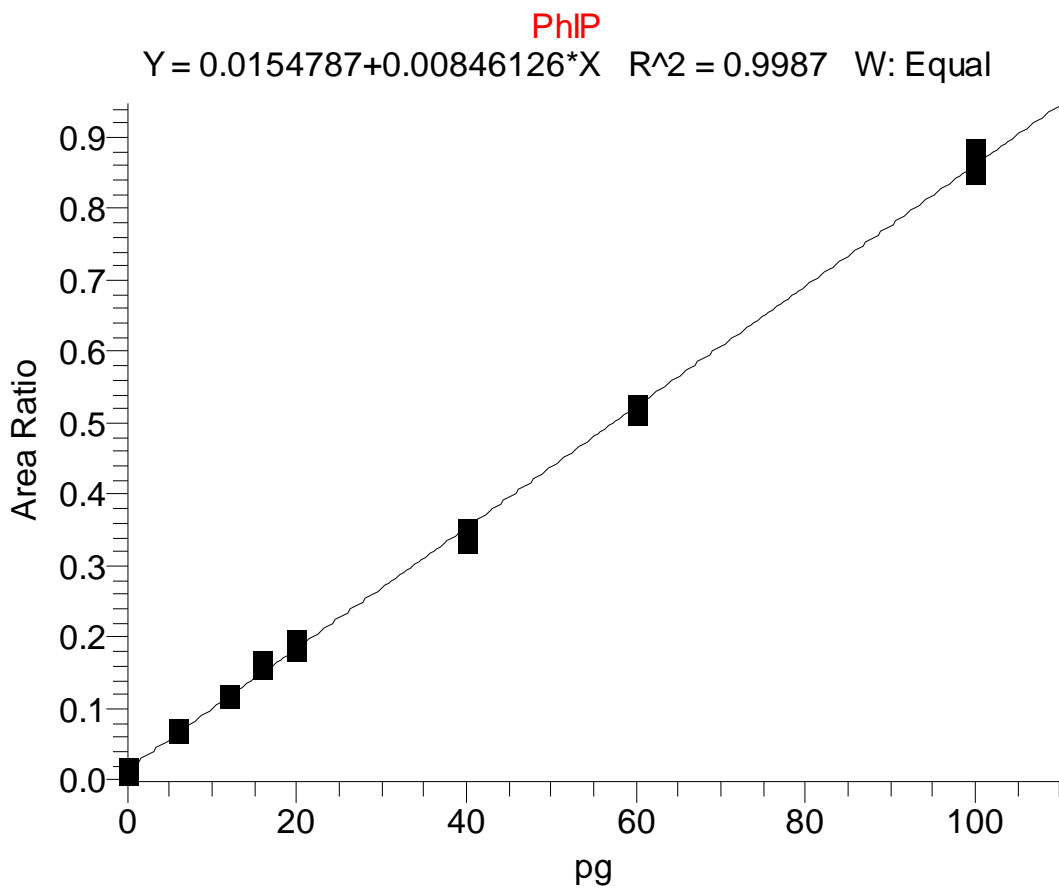
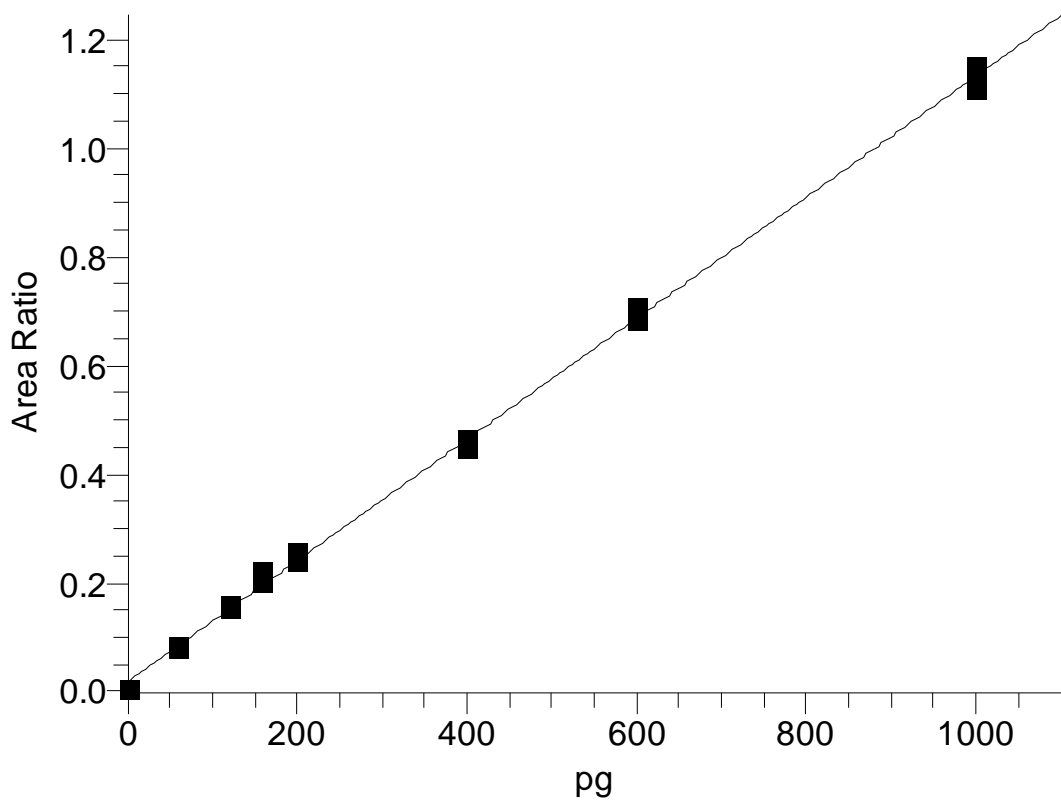


Figure S-3A – S-3D. Calibration curves of PhIP and its metabolites



HONPhIPN3GI

$$Y = 0.0178683 + 0.00111477 * X \quad R^2 = 0.9988 \quad W: \text{Equal}$$



PhIPN3GI

$$Y = 0.010751 + 0.000965815 * X \quad R^2 = 0.9992 \quad W: \text{Equal}$$

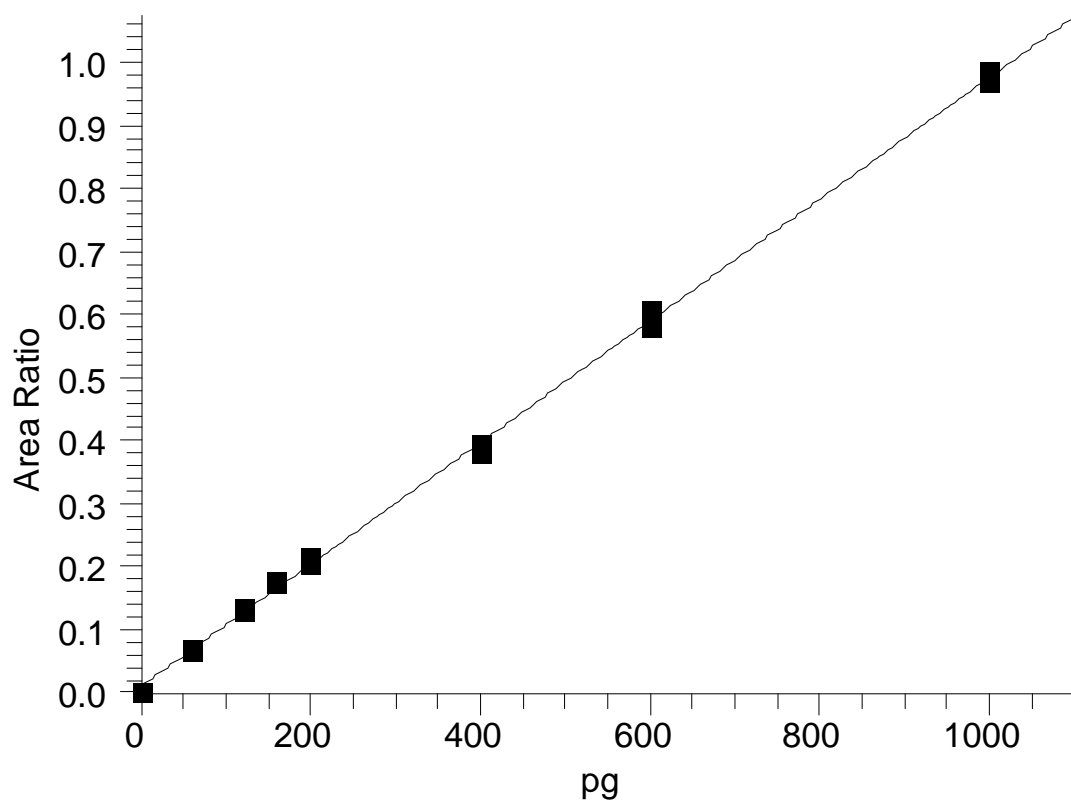
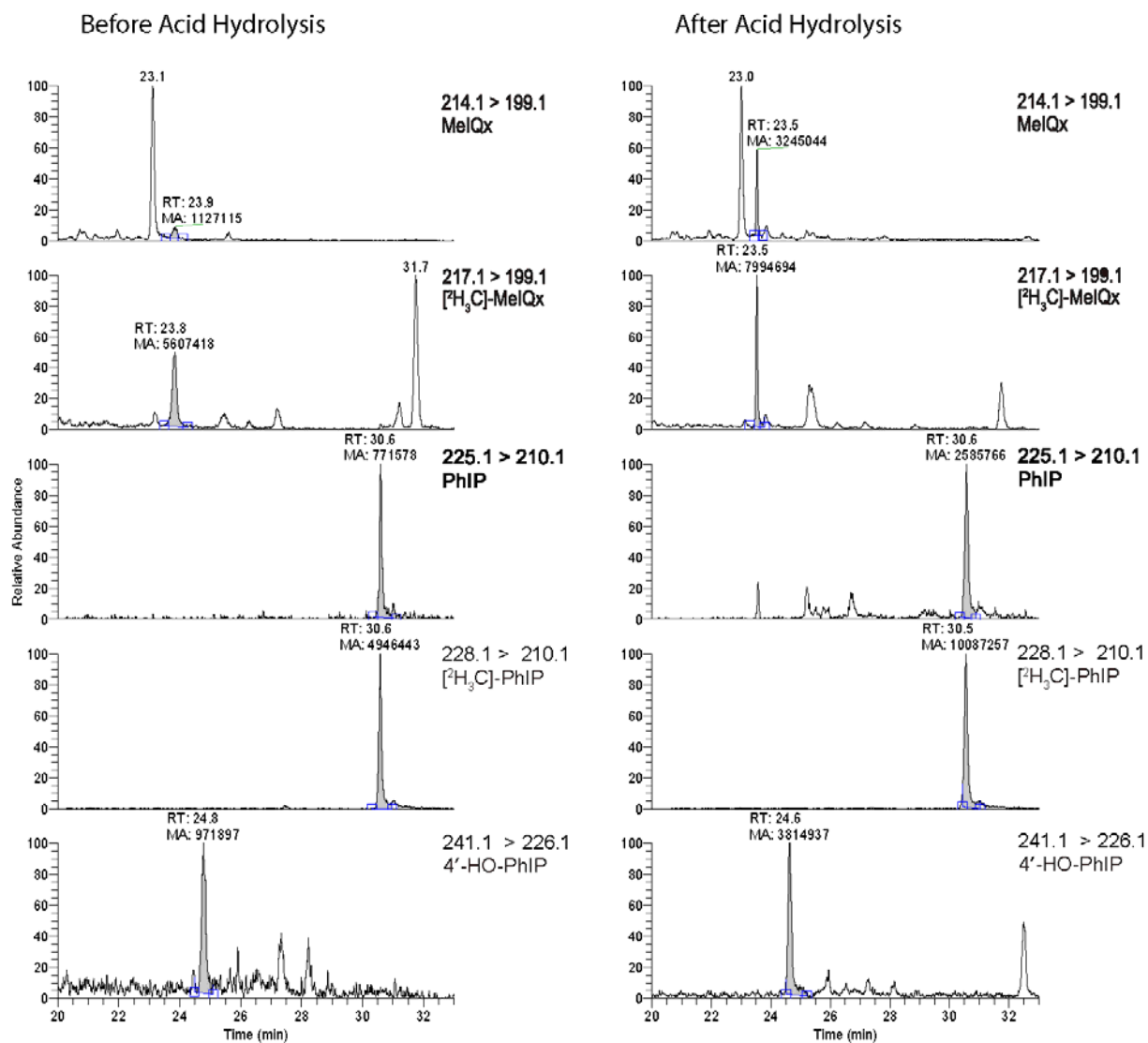


Figure S-4. LC-ESI/MS/MS traces of MeIQx, PhIP, and 4'-HO-PhIP in urine of an omnivore, before and after acid hydrolysis of urine



References

- (1) Styczynski, P. B., Blackmon, R. C., Groopman, J. D., and Kensler, T. W. (1993) The direct glucuronidation of 2-amino-1-methyl-6-phenylimidazo[4,5-b]pyridine (PhIP) by human and rabbit liver microsomes. *Chem. Res. Toxicol.* 6, 846-851.